

Keywords: aldo-keto reductase 1C3; inhibitors; leukaemia

# Selective AKR1C3 inhibitors do not recapitulate the anti-leukaemic activities of the pan-AKR1C inhibitor medroxyprogesterone acetate

F Khanim<sup>1,8</sup>, N Davies<sup>2,8</sup>, P Veliça<sup>3</sup>, R Hayden<sup>1</sup>, J Ride<sup>1</sup>, C Pararasa<sup>4</sup>, M G Chong<sup>2</sup>, U Gunther<sup>2</sup>, N Veerapen<sup>1</sup>, P Winn<sup>5</sup>, R Farmer<sup>5</sup>, E Trivier<sup>6</sup>, L Rigoreau<sup>6</sup>, M Drayson<sup>7</sup> and C Bunce<sup>\*,1</sup>

<sup>1</sup>School of Biosciences, University of Birmingham, Birmingham B15 2TT, UK; <sup>2</sup>School of Cancer Sciences, University of Birmingham, Birmingham B15 2TT, UK; <sup>3</sup>Haematology Department, UCL Cancer Institute, London WC1E 6DD, UK; <sup>4</sup>School of Life and Health Sciences, Aston University, Birmingham B4 7ET, UK; <sup>5</sup>Centre for Systems Biology, University of Birmingham, Birmingham B15 2TT, UK; <sup>6</sup>CRT Discovery Laboratories, Babraham, Cambridge CB22 3AT, UK and <sup>7</sup>Immunity and Infection, University of Birmingham, Birmingham B15 2TT, UK

**Background:** We and others have identified the aldo-keto reductase AKR1C3 as a potential drug target in prostate cancer, breast cancer and leukaemia. As a consequence, significant effort is being invested in the development of AKR1C3-selective inhibitors.

**Methods:** We report the screening of an in-house drug library to identify known drugs that selectively inhibit AKR1C3 over the closely related isoforms AKR1C1, 1C2 and 1C4. This screen initially identified tetracycline as a potential AKR1C3-selective inhibitor. However, mass spectrometry and nuclear magnetic resonance studies identified that the active agent was a novel breakdown product (4-methyl(de-dimethylamine)-tetracycline (4-MDDT)).

**Results:** We demonstrate that, although 4-MDDT enters AML cells and inhibits their AKR1C3 activity, it does not recapitulate the anti-leukaemic actions of the pan-AKR1C inhibitor medroxyprogesterone acetate (MPA). Screens of the NCI diversity set and an independently curated small-molecule library identified several additional AKR1C3-selective inhibitors, none of which had the expected anti-leukaemic activity. However, a pan AKR1C, also identified in the NCI diversity set faithfully recapitulated the actions of MPA.

**Conclusions:** In summary, we have identified a novel tetracycline-derived product that provides an excellent lead structure with proven drug-like qualities for the development of AKR1C3 inhibitors. However, our findings suggest that, at least in leukaemia, selective inhibition of AKR1C3 is insufficient to elicit an anticancer effect and that multiple AKR1C inhibition may be required.

Members of the aldo/keto reductase (AKR) superfamily catalyse the conversion of aldehydes and ketones to their corresponding alcohols by utilising NADH and/or NADPH as cofactors. We and others have identified AKR1C3 as a potentially novel therapeutic target in prostate cancer, breast cancer and leukaemia (Desmond

*et al*, 2003; Byrns and Penning, 2009; Houghton *et al*, 2011; Byrns *et al*, 2012; Mitsiades *et al*, 2012). Our studies in acute myeloid leukaemia (AML) have demonstrated that enforced AKR1C3 overexpression represses the *all-trans* retinoic acid (ATRA)-induced differentiation of HL-60 AML cells (Desmond *et al*, 2003),

\*Correspondence: Professor C Bunce; E-mail: C.M.Bunce@bham.ac.uk

<sup>8</sup>Equal first authors.

Revised 3 January 2014; accepted 13 January 2014; published online 25 February 2014

© 2014 Cancer Research UK. All rights reserved 0007–0920/14

whereas conversely knockdown of AKR1C3 in K562 cells results in erythroid differentiation (Birtwistle *et al*, 2009). We have also shown that the known AKR inhibitors, indomethacin and medroxyprogesterone acetate (MPA), promote the differentiation and apoptosis of AML cells (Bunce *et al*, 1994; Khanim *et al*, 2009a). More recently, we have demonstrated that MPA in combination with bezafibrate (BEZ) has *in vivo* clinical activity against AML (Murray *et al*, 2010). We have therefore proposed AKR1C3 as a novel regulator of myeloid cell differentiation and a potential new therapeutic target in leukaemia.

The role of AKR1C3 in prostate and breast cancer has been predominantly inferred by virtue of altered mRNA and/or protein expression levels in tumour tissues and in association with disease progression (Agung *et al*, 2005; Suzuki *et al*, 2005; Hofland *et al*, 2010; Beckmann *et al*, 2011; Aderibigbe *et al*, 2012; Jamieson *et al*, 2012), and the enzyme's recognised 3,α- and 17,β-hydroxysteroid activities and 9,α-11,β prostaglandin D2 (9α, 11β-PGD<sub>2</sub>) dehydrogenase activity (Matsuura *et al*, 1998; Kuhne *et al*, 2001; Byrns and Penning, 2009; Byrns *et al*, 2012). Byrns *et al* (2012) demonstrated that overexpression of AKR1C3 in LNCaP prostate cancer cells resulted in increased testosterone production and resistance to finasteride. Single-nucleotide polymorphisms in AKR1C3 have been associated with disease progression and aggressiveness in prostate carcinomas (Izumoto *et al*, 2005; Richards *et al*, 2006). AKR1C3 polymorphisms have also been shown to modulate the risk of other cancers, including bladder cancer, childhood leukaemias and diffuse large B-cell lymphoma (Bauman *et al*, 2004; Morakinyo *et al*, 2011; Adegoke *et al*, 2012c). Separately, it has been shown that AKR1C3 can inactivate and induce resistance to the anticancer drugs doxorubicin, oracin and cisplatin (Adegoke and Nyokong, 2012; Adegoke *et al*, 2012a, b), whereas elevated AKR1C3 protein levels were associated with radioresistance in non-small cell lung carcinomas (Jamieson *et al*, 2012).

AKR1C3 belongs to a highly conserved AKR subfamily (in humans AKR1C1, -1C2, -1C3 and -1C4), which displays differential tissue expression and possess overlapping but differing pleiotropic activities (Kuhne *et al*, 2001; Gratacos-Cubarsi *et al*, 2007; Birtwistle *et al*, 2009; Velica *et al*, 2009; Rizner and Penning, 2013). MPA does not display strong AKR1C3 selectivity amongst this family and only inhibits AKR1C3 at doses higher than those used for its respective primary indications as a contraceptive steroid. These considerations have driven many research groups to search for lead compounds with a greater selectivity towards AKR1C3 that could be developed as novel cancer therapies (Halling-Sorensen *et al*, 2002; Ghia *et al*, 2003; Qiu *et al*, 2007; Zargar *et al*, 2011; Burnett *et al*, 2012; Giebel *et al*, 2013; Hebert *et al*, 2013; Wasylshen *et al*, 2013). In recognition of this, several laboratories have undertaken structural studies of AKR1C3 bound to inhibitors and substrates and embarked on the identification of lead compounds for drug development (Zargar *et al*, 2011; Burnett *et al*, 2012; Hebert *et al*, 2013; Wasylshen *et al*, 2013).

New drug development is challenging and as the pharmacologist and Nobel laureate James Black is quoted as saying, 'the most fruitful basis for the discovery of a new drug is to start with an old drug'. In order to screen existing drugs for greater selective AKR1C3 inhibition, we developed a high-throughput assay of AKR1C1, -1C2, -1C3 and -1C4 activity based on the consumption of NADPH in the presence of the pan-AKR substrate phenanthrenequinone (PQ) (AKR1C-diaphorase assay). An initial screen of an in-house custom-built library of 100 off-patent drugs (FMC1) identified tetracycline as a potential AKR1C3-selective inhibitor. However, mass spectrometry and nuclear magnetic resonance (NMR) studies identified that the active agent was in fact a novel tetracycline breakdown product (4-methyl(de-dimethylamine)-tetracycline (4-MDDT). We demonstrate here that this novel agent enters AML cells and inhibits the AKR1C3

activity within, but unexpectedly does not recapitulate the anti-leukaemic actions of the pan-AKR1C3 inhibitor MPA either alone or in combination with BEZ. Further screens of the NCI diversity set (<http://dtp.cancer.gov>) and of a small-molecule library curated at the Cancer Research Technology (CRT) identified several additional AKR1C3-selective inhibitors. Importantly, none of these AKR1C3-selective compounds had anti-leukaemic activity. However, a pan AKR1C1, -1C2, -1C3 inhibitor also identified in the NCI diversity set faithfully recapitulated the actions of MPA.

## MATERIALS AND METHODS

**FMC100 drug library.** All drugs were purchased from Sigma-Aldrich (Poole, UK). Stocks were prepared at 10 000 × reported peak serum concentrations in dimethylsulphoxide DMSO, ethanol or water and stored at -20 °C. Tetracycline hydrate (Sigma-Aldrich) was prepared at 225 mM in DMSO.

**National cancer institute diversity set.** NCI compounds were ordered from the NCI/DTP Open Chemical Repository (<http://www.dtp.nci.nih.gov>). Stocks were prepared as 10 mM in DMSO in 96-well plates and stored at -20 °C.

**Cancer research technologies (CRT).** A1, A6 and A9 were identified as AKR1C3-selective inhibitors by CRT using a fluorescence-based assay and purified recombinant AKR1C1-4 proteins (Hebert *et al*, 2013). Compounds A1((CRT0036521) 3-(3,4-dihydro-1H-isoquinoline-2-sulphonyl)-benzoic acid), A6 ((CRT0083914) 1-[4-(2-methyl-piperidine-1-sulphonyl)-phenyl]-pyrrolidin-2-one), and A9 ((CRT0093964) [4-(4-chloro-phenyl)-piperazin-1-yl]-morpholin-4-yl-methanone)(Figure 7A), were provided as 12–15 mM stocks in anhydrous DMSO and stored at 4 °C.

**Production and purification of recombinant AKR1C proteins.** N-terminally His<sub>6</sub>-tagged recombinant AKR1C1, 2, 3 and 4 were cloned into pET28b vectors (Novagen, Darmstadt, Germany) and expressed and purified as previously described (Lovering *et al*, 2004; Davies *et al*, 2009).

**High-throughput recombinant AKR1C-diaphorase assay.** Supplementary Figure 1 shows a schematic for the fluorometric AKR1C activity assay using PQ. Compounds were screened against purified recombinant AKR1C1, 2, 3 and 4 proteins in duplicate wells of 96-well plates. In the first step, reactions contained 4 μM PQ, 5 μM β-NADPH, 15 μg recombinant AKR1C (recAKR1C) protein and 100 μM test compound in 50 mM potassium phosphate buffer (pH 6.5). Dimethylsulphoxide and acetonitrile were both present at 2% (v/v) each. Negative, positive and no-inhibitor control wells were set in duplicate on each plate; negative control had no PQ, while the positive controls used 5 μM MPA or 20 μM indomethacin. The assay as used measured uncompetitive inhibition owing to the formation of the E-NADP + -I complex (Byrns *et al*, 2012). PQ was non-limiting in this assay as the product spontaneously oxidises back to PQ, as determined by the restoration of the initial rate of NADPH consumption when NADPH was re-added to the assay (Supplementary Figure 1B). Plates were incubated at 37 °C for 15 min before resazurin and diaphorase were added to final concentrations of 26.8 mM and 0.54 U/ml, respectively. The contents of wells were mixed by repeated pipetting and plates incubated for a further 10 min at 37 °C. Fluorescence was measured (EX<sub>530 nm</sub>/EM<sub>595 nm</sub>) in a fluorimeter (Bio-Tek Instruments, Winooski, VT, USA) using the KC4 software (BioTek, Potten, UK). Dose titration experiments to calculate IC<sub>50</sub> values were performed as above. Percentage enzyme activity was calculated using  $100 - (100 \times (R - B1) / (B0 - B1))$ , where *R* is A530/590 of well with test compound, *B1* is average of A530/590 of duplicate wells without compound and *B0* is average A530/590 reading of duplicate wells without substrate.

**NADPH assay for AKR1C enzymatic activity.** Assays for all four human recombinant AKR1C enzymes were performed, as described previously (Davies *et al*, 2009).

**HPLC purification of tetracycline breakdown product 4-MDDT.** 4-MDDT was purified at room temperature using a Dionex DX-600 HPLC system (Thermo Scientific, Hemel Hempstead, UK), Prevail Select C18 5  $\mu$  (250 mm  $\times$  4.6 mm i.d.) HPLC column. Elution at a flow of 1 ml/min was performed with a linear gradient between solvent A (50% methanol:0.1% trifluoroacetic acid v/v) and solvent B (98% methanol:0.1% trifluoroacetic acid v/v). Peak identification was performed by comparing spectra

(collected between 220 and 500 nm). Fractions were collected, dried down under nitrogen stream and 4-MDDT resuspended in DMSO at 50 mM using its molecular mass as 413, as measured by GC-MS analysis (see below).

**Mass spectrometry and NMR.** Mass spectrometry to define mass was performed by Dr Peter Ashton (School of Chemistry, University of Birmingham) on both freshly prepared tetracycline and HPLC-purified tetracycline derivative (4-MDDT) by electrospray mass spectrometry analysis, scanning for molecules with RMM 200–2000.

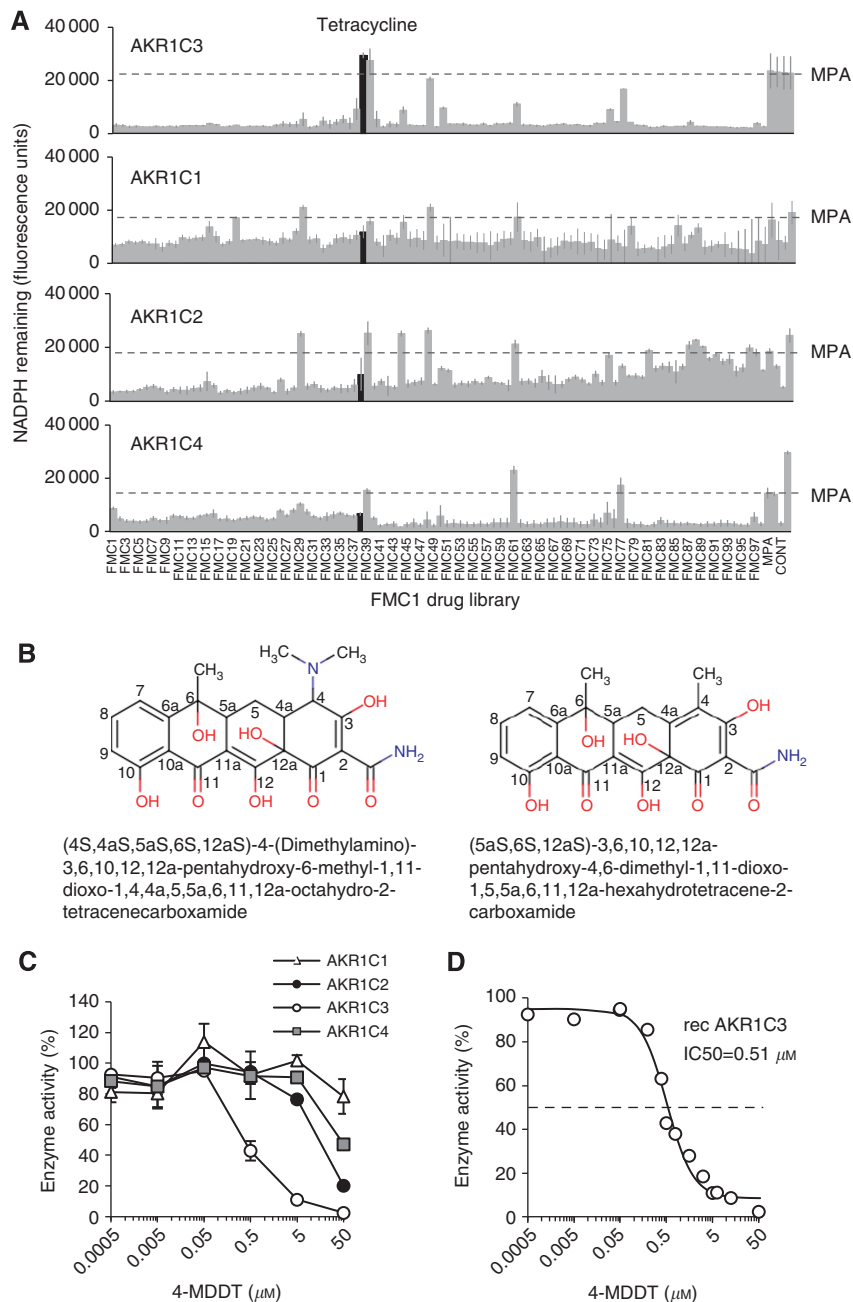


**Figure 1.** Identification of a novel tetracycline breakdown product. **(A)** A panel of 100 clinically licensed drugs (FMC100) at peak serum concentrations was screened for AKR1C-inhibitory activity against recombinant purified AKR1C proteins using the AKR1C-diaphorase assay. Data shown is mean fluorescence arbitrary units. Black bars indicate tetracycline and the dashed line represents level of inhibition by 5  $\mu$ M MPA. GC-MS and NMR were used to elucidate the structure of the novel tetracycline breakdown product 4-methyl,(didemethyl)-tetracycline (4-MDDT). **(B)** Structures and names of the parent tetracycline and novel tetracycline breakdown product. **(C)** The isoform specificity of HPLC-purified 4-MDDT was determined against recombinant AKR1C proteins using the AKR1C-daphorase assay (see Materials and Methods). **(D)** The IC<sub>50</sub> of 4-MDDT for recombinant AKR1C3 protein was determined using the PQ assay (see Materials and Methods).

To elucidate the structure, 1D and 2D NMR experiments were performed on both 10 mM freshly prepared tetracycline and HPLC-purified tetracycline derivative (4-MDDT). Spectra were recorded on a Bruker 500 MHz spectrometer (Bruker, Coventry, UK) and a Bruker 600 MHz spectrometer (Bruker), both equipped with cryogenically cooled probes. All spectra were recorded at a temperature of 300 K, in either  $d_6$ -DMSO or  $d_3$ -acetonitrile. One-dimensional  $^1\text{H}$  NMR spectra were acquired using a spectral width of 7.2 kHz and 32 K data points. One-dimensional  $^{13}\text{C}$  NMR spectra were obtained using a spectral width of 24 kHz with 64 K data points. One-dimensional  $^{15}\text{N}$  NMR spectra were obtained using a spectral width of 25 kHz with 32 K data points. For further assignments verification, 2D COSY, TOCSY (100 ms mixing time) and NOESY (200 ms mixing time) spectra were obtained, along with  $^{13}\text{C}$ -HSQC and  $^{15}\text{N}$ -HSQC (with the INEPT delay adjusted for short and for long-range couplings) in order to identify NH and  $\text{N}(\text{CH}_3)_2$  groups.

**In silico docking studies.** Simulated docking of tetracycline and 4-MDDT into AKR1C3 (PDB ID 1S2C with flufenamic acid removed) was performed using Autodock 4.2 (Wu *et al.*, 2010). The coordinates of tetracycline with  $\text{Mg}^{2+}$  were adapted from the

crystal structure PDB ID 2TCT. The coordinates of 4-MDDT were calculated by editing the tetracycline coordinates using PyMol. UCSF Chimera 1.6.2 (Li *et al.*, 2010) was used to calculate AM-1 BCC charges for ligands in different proton configurations with/without  $\text{Mg}^{2+}$ . Polar hydrogen atoms and partial charges for the protein and NADPH cofactor were calculated using the standard settings in MGLTools. The input and output files for Autodock were processed using the standard MGLTools scripts. The centre of the docking site was the average coordinate of the flufenamic acid bound in PDB 1S2C.

A number of calculations included some flexibility of the AKR1C3 structure by allowing torsional rotation of residues having the most contact with the ligand (ASN167, PHE306, PHE311, TYR216, TRP227, LEU54, LEU128, SER129, LEU122, TRP86, MET120). In addition, the two magnesium-bound 4-MDDT configurations were docked with the same flexible residues as above but removing TYR216 and MET120 from the list and adding ARG226.

**Cell culture and drug treatments.** HL60, KG1a and K562 (ATCC) cell lines were maintained in RPMI-1640 medium with L-glutamine supplemented with 10% v/v heat-inactivated

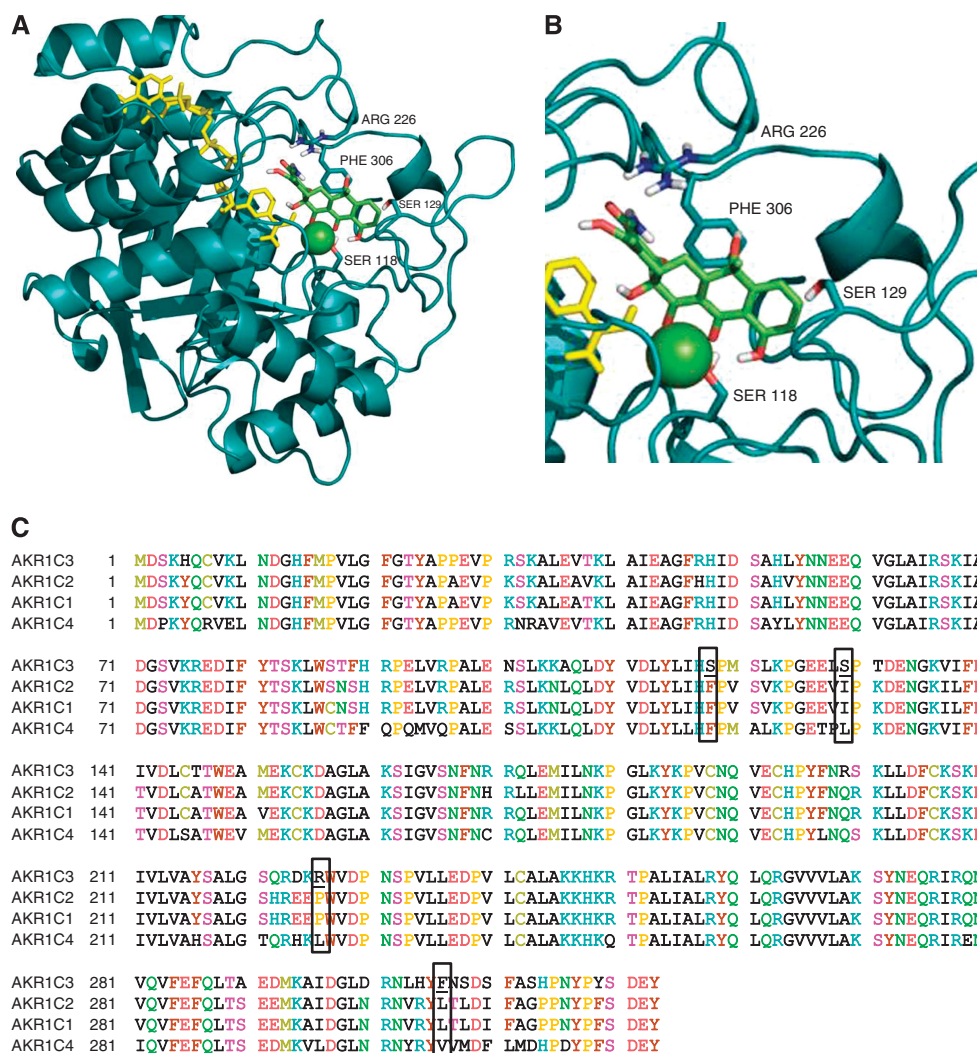


**Figure 2.** *In silico* docking of 4-MDDT into the crystal structure of AKR1C3. (A) Autodock was used to dock 4-MDDT into our previously published AKR1C3 crystal structure after flufenamic acid was removed (PDB ID 1S2C)[39]. The 4-MDDT is coloured by atom type (green: carbon, red: oxygen, white: hydrogen) and shown as sticks, with magnesium a green sphere. The  $\text{NADP}^+$  cofactor is coloured yellow and the protein is rendered as an aquamarine cartoon ribbon. Side chains identified as potentially providing specificity are shown as sticks and labelled. (B) Close-up of the predicted binding sites and key interacting amino-acid residues. (C) Protein Sequence alignment of AKR1C1-4 with the key interacting amino-acid residues highlighted in boxes.

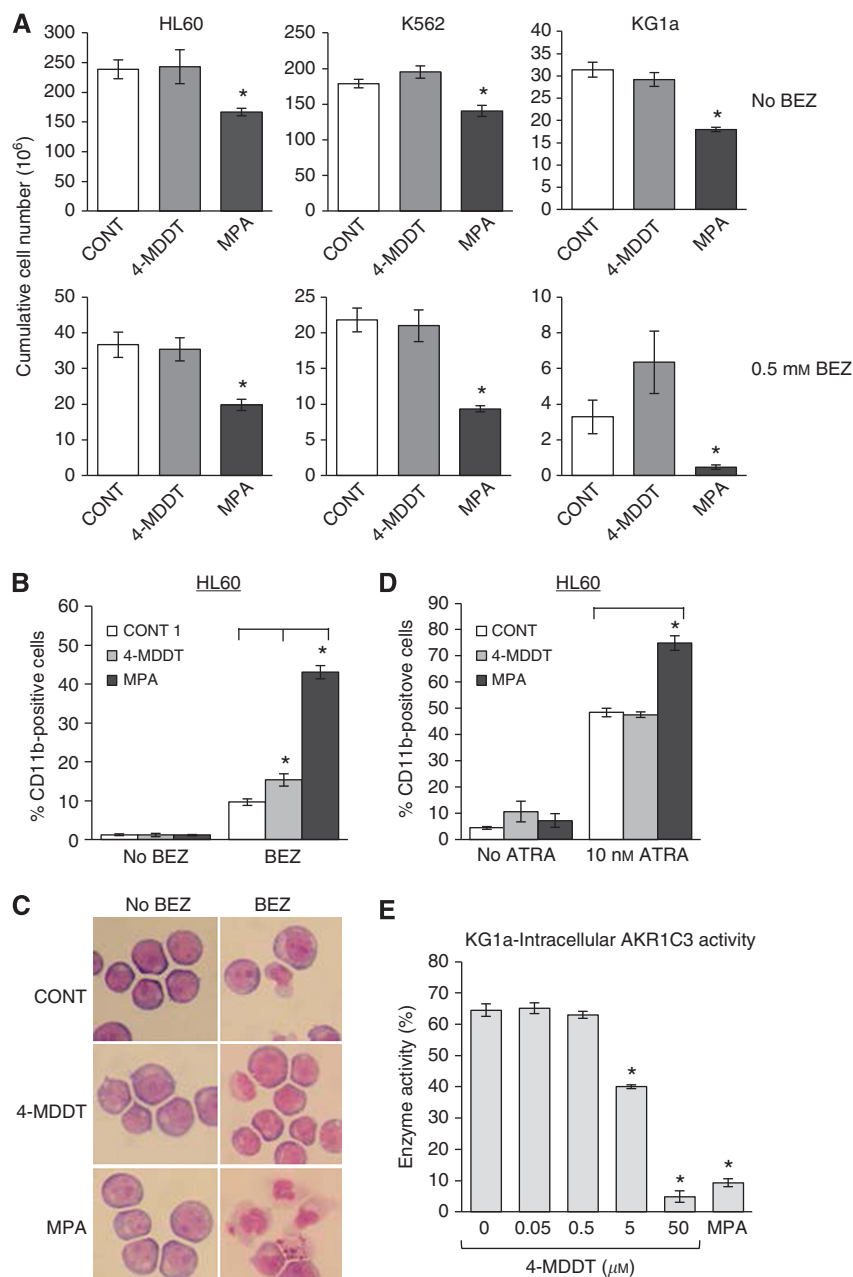


**Figure 3.** 4-MDDT does not recapitulate the actions of MPA against AML cell lines. HL-60, K562 and KG1a cells were treated for 7 days with either solvent control, 50 μM 4-MDDT or 5 μM MPA, alone or in combination with 0.5 mM BEZ. **(A)** Cumulative cell counts for HL60, K562 and KG1a after 7 days treatment. Data shown is mean of a minimum of  $N=3$  experiments  $\pm$  s.e.m. **(B and D)** HL60 differentiation was assessed at day 7 by staining for CD11b and flow cytometry following treatment with either solvent control, 50 μM 4-MDDT or 5 μM MPA with or without 0.5 mM BEZ or 10 nM ATRA. Data shown is mean of a minimum of  $N=3$  experiments  $\pm$  s.e.m. **(C)** Cytopsin of HL60 cells treated for 7 days as described above were stained with Jenner–Giemsa to demonstrate changes in cell morphology. **(E)** Intracellular AKR1C3 11β-prostaglandin reductase activity in KG1a cells was assessed in the presence of a dose titration of 4-MDDT or 5 μM MPA using <sup>3</sup>H-PGD<sub>2</sub> and thin layer chromatography. Data shown is mean of  $N=4$  experiments  $\pm$  s.e.m. \* $P<0.01$ .

fetal bovine serum and penicillin (100 units/ml)/streptomycin (100 μg/ml) (all from Gibco, Invitrogen Ltd, Paisley, UK) at 37 °C with 5% CO<sub>2</sub>. Cells were passaged every 2 days maintaining cell densities between  $0.25\text{--}1.5 \times 10^6$  cells/ml. Drug treatments in 96-well plate assays were performed using  $1 \times 10^4$  cells/well in 200 μl, or in flasks at  $0.25 \times 10^6$  cells/ml in 4 ml media. Appropriate volumes of DMSO and/or ethanol were added as solvent controls in control treatments.

**Chronic lymphocytic leukaemia (CLL) cells.** Chronic lymphocytic leukaemia blood samples were obtained from unselected patients

diagnosed with CLL, according to standard morphologic, immunophenotypic and clinical criteria, attending the outpatient clinic at Birmingham Heartlands Hospital following informed written consent for the study, which had received local ethical approval. Primary mononuclear cells were prepared using Ficoll Paque-Plus (Anachem, Luton, UK) as previously described. Resultant cells were cultured and treated in a 96-well plate co-culture system, with L-control fibroblasts, as described previously (Hayden *et al*, 2010). Viability was assessed at 24 h using annexin V and propidium iodide staining, and flow cytometry (Hayden *et al*, 2010).

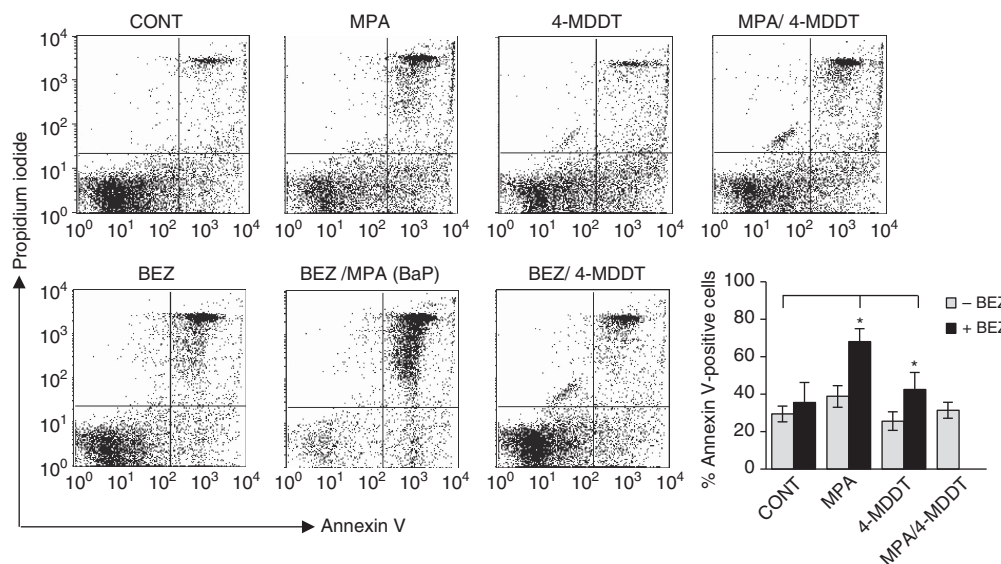


**Figure 4.** 4-MDDT does not recapitulate the actions of MPA against primary CLL cells. Peripheral blood mononuclear cells from CLL patients were cultured on non-CD40L-expressing stroma in a ratio of 10:1 in 96-well plates. Treatments with either solvent control, 0.5 mM BEZ, 5  $\mu$ M MPA, BEZ/MPA (BaP), 5.1  $\mu$ M 4-MDDT, MPA/4-MDDT or BEZ/4-MDDT were performed in triplicate for 24 h, before harvesting and staining with Annexin V (AV) and propidium iodide (PI), and analysis by flow cytometry. Plot shown is for  $n = 4$  samples + s.e.m.

**$^3\text{H}$ -PGD<sub>2</sub> turnover analysis by thin layer chromatography.** AKR1C3-mediated PGD<sub>2</sub> turnover in intact cells was determined by thin layer chromatography as described previously (Desmond *et al*, 2003; Davies *et al*, 2009).

**Measurement of cell viability.** HL60, KG1a and K562 cell viability was measured using manual counts, or by flow cytometry on a BD FACSCalibur utilising Cell Quest Pro software (Becton Dickinson, Plymouth, UK), viable gates and fluorescent Cytocount beads (DakoCytomation, Ely, UK).

**Assessment of cell differentiation.** HL-60 cells were treated for 7 days with re-feeding and re-treating every 2 days. Differentiation was assessed by flow cytometry (Becton Dickinson FACS Calibur and Becton Dickinson Cell Quest software) using PE-CD11b (Becton Dickinson).

**Jenner–Giemsa staining of slides.** Cytospins were prepared from 75–100  $\mu$ l of culture. Slides were air dried, methanol fixed and stained as described previously (Khanim *et al*, 2009a).

## RESULTS

The four human AKR1C enzymes share greater than 86% amino-acid sequence identity and, also share overlapping substrate promiscuities (Deyashiki *et al*, 1994; Dufort *et al*, 1996; Velica *et al*, 2009). Thus identifying inhibitors selective for individual enzymes from this subfamily represents a considerable challenge. To this end we have developed a readily accessible indirect AKR1C fluorescence-based assay that can be used for high-throughput screening (Supplementary Figure 1). The assay utilises the pan-human AKR1C substrate PQ and NADPH as cofactors and measures AKR1C activity indirectly by determining levels of NADPH remaining in the presence or absence of inhibitor (Supplementary Figure 1).

As part of our drug redeployment strategy in leukaemia and lymphoma, we have assembled a library (FMC1) of 100 off-patent commonly used drugs of a known toxicological profile. This library has been constructed to reflect each of the drug's peak serum concentration and differs from other libraries that normally

contain drugs at a common arbitrary concentration. The FMC1 library was screened initially at 10  $\times$  peak serum concentrations against recombinant AKR1C1, -1C2, -1C3 and -1C4 using the AKR1C-diaphorase-based assay (Figure 1). Indomethacin and MPA were included as control inhibitors. Wells were included containing enzyme and no inhibitor (+ve control) and without enzyme or inhibitor (-ve control). This screen identified the broad-spectrum polyketide antibiotic tetracycline as a potential AKR1C3-selective inhibitor (Figure 1A).

Tetracycline is known to be unstable with factors such as light, temperature, and pH strongly affecting its chemical stability (Bagga *et al*, 2005; Patriciu *et al*, 2005; Feng *et al*, 2006). Under alkaline conditions, tautomerisation, demethylation, and the formation of terranoic acid and isoforms have been described (Guan and Xiong, 2011). Under acidic conditions, epimerisation reactions of tetracyclines take place (Patriciu *et al*, 2005; Wang *et al*, 2010) to give 4-epimeric, anhydrous,  $\alpha/\beta$  apo, and ter forms (Guan and Xiong, 2011). As the solution of tetracycline hydrate in DMSO being tested was observed to change colour within a few days, the solution was subjected to reverse-phase HPLC analysis that revealed the rapid conversion of the dissolved tetracycline to an unknown breakdown product. Freshly prepared tetracycline solutions demonstrated no AKR1C3-inhibitory activity; the AKR1C3-selective activity of the stored solution was shown to be due to the breakdown product, the presence of which was confirmed by column chromatography. The purified tetracycline breakdown product was analysed by MS to give a suggested  $M_r$  of 413, which differed by  $\sim 31$  Da from the actual mass of tetracycline (444.43 Da). This tetracycline breakdown moiety was subjected to NMR analysis of its structure, which identified a substitution at carbon 4 replacing the dimethylamino group with a methyl group (Figure 1B; Supplementary Tables 1–3). Searches of several databases ([www.chemspider.com](http://www.chemspider.com), <http://pubchem.ncbi.nlm.nih.gov>) did not identify any other tetracycline derivatives with a similar structure. Hence, to our knowledge this is the first description of this tetracycline derivative that we have termed 4-methyl,(didemethyl)-tetracycline (4-MDDT) to distinguish from the 4-dimethylamino,6-methyl-tetracycline parent molecule. Analysis of the purified compound in the AKR1C-diaphorase assay confirmed that the selective AKR1C3-inhibitory activity resided in

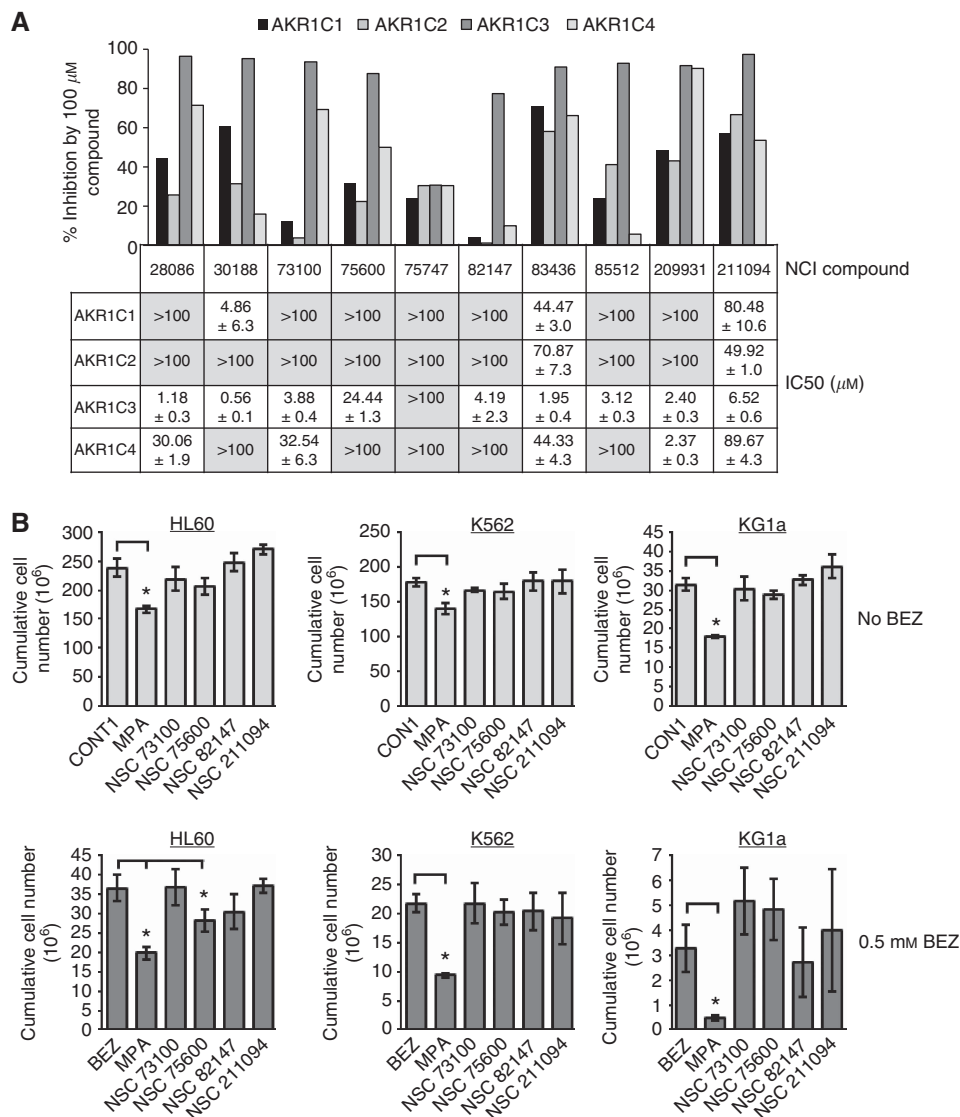


**Figure 5. Identification of AKR1C3-selective inhibitors from the NCI Diversity Set. (A)** NCI compounds were screened against recombinant AKR1C proteins using the AKR1C-diaphorase assay (see Materials and Methods) and % inhibition of activity measured. IC<sub>50</sub>s of selected compounds against all four AKR1C isoforms, shown below the bar chart, were calculated using dose titrations of each compound against recombinant AKR1C protein in the NADPH assay. **(B)** Cumulative cell counts for HL60, K562 and KG1a after 7 days treatment with either solvent control, 5  $\mu$ M MPA, or the selected compounds at 10 times the IC<sub>50</sub> concentration, without (top three panels) or with 0.5 mM BEZ (bottom three panels). Data shown is mean of a minimum of  $N=3$  experiments  $\pm$  s.e.m. \* $P<0.01$ .

the 4-MDDT derivative (Figure 1C) and not the parent compound and had an IC<sub>50</sub> of 0.51  $\mu$ M (Figure 1D). 4-MDDT is more stable compared with the parent compound.

To interrogate the basis of the specificity of 4-MDDT for AKR1C3, we performed ligand-protein docking calculations using our published AKR1C3 structure (Figure 2) (Lovering *et al*, 2004). Given the uncertain proton configuration and the flexibility of both ligand and protein, we did not anticipate finding the exact binding orientation of 4-MDDT in the active site but anticipated some insights into ligand specificity. Tetracycline is generally found associated with a magnesium ion, so we performed docking experiments both in the presence and absence of magnesium to determine if this affected the analysis. Our calculations indicate that magnesium-bound tetracycline is too large for the active site of the AKR1C3 crystal structure, whereas magnesium-bound 4-MDDT fits (Figure 2). This discrimination was less obvious for non-magnesium-bound ligands. Given the experimental data, this would seem to support the binding of 4-MDDT with a

bound magnesium. With regard to understanding AKR1C3 selectivity, the docked 4-MDDT contacted residues of AKR1C3 that differ greatly in physicochemical properties from those of the other AKR1C subfamily members, notably S118 (c.f. F), S129 (c.f. I/L), R226 (c.f. P/L) and F306 (c.f. L/V) (Figure 2B). Given the otherwise highly similar sequences between the AKR1C isoforms (Figure 2C), we might anticipate these residues in AKR1C3 to be of significance. However, a detailed description of the mechanism of 4-MDDT selectivity for AKR1C3 will require detailed crystallography studies.

We next turned to investigating the action of 4-MDDT against HL-60, K562 and KG1a AML cell lines. As previously described (Khanim *et al*, 2009a), 5  $\mu$ M MPA alone had a moderate but statistically anti-proliferative effect on all three AML cell lines and greatly enhanced AML cell killing when combined with BEZ (Figure 3A). In contrast, 50  $\mu$ M 4-MDDT did not display these activities (Figure 3A). We also previously demonstrated that the action of BEZ and MPA (BaP) against K562 and KG1a cells was

mediated by direct cell killing but that in the case of HL-60 cell death was preceded by the onset of cell differentiation (Khanim *et al*, 2009b). Here, we again observed that MPA, when combined with BEZ, strongly promoted HL-60 cell differentiation as measured by expression of CD11b and phenotypic changes (Figure 3B and C). However, the effect of 4-MDDT was very much reduced (Figure 3B and C). Finally, as previously observed, MPA promoted the differentiation of HL-60 cells in response to ATRA but again 4-MDDT did not (Figure 3D). The failure of 4-MDDT to exert MPA-like activities were not due to a failure to enter cells and inhibit AKR1C3 as demonstrated by the inhibition of intracellular  $11\beta$ -PGD<sub>2</sub>-ketoreductase activity in KG1a cells (Figure 3E).

Our previous studies demonstrated that the anti-leukaemic actions of MPA, when combined with BEZ, extended to CLL cells (Hayden *et al*, 2009). We therefore tested 4-MDDT alone and in combination with BEZ or MPA against four primary CLL samples. As previously reported, neither BEZ nor MPA as single agents markedly increased apoptosis of CLL cells, but the combination (BaP) markedly increased apoptosis. Similarly 4-MDDT had little effect against CLL cells but unlike MPA did not induce apoptosis when combined with BEZ (Figure 4).

These findings suggested that inhibition of AKR1C3 alone is not adequate to exert an anti-leukaemic effect. To further test this hypothesis, we screened a large panel of small chemical compounds from the NCI diversity set for alternative AKR1C3-selective inhibitors using the AKR1C-diaphorase assay. The IC<sub>50</sub> values of compounds demonstrating AKR1C3 selectivity against all AKR1C isoforms was measured using the NADPH assay. As shown in Figure 5A, this screen identified 10 compounds that showed varying degrees of AKR1C3-selective inhibition. Four of these compounds were selected for analysis of their actions against HL-60, K562 and KG1a cells when used alone and when in combination with BEZ (Figure 5B; Supplementary Figure 2). As in the case of 4-MDDT, none of the NCI compounds matched the anti-proliferative actions of MPA and none accentuated cell killing in the presence of BEZ (Figure 5B). An independent screen,

using an alternative assay (Hebert *et al*, 2013), of the CRT small-molecule library identified three distinct chemical series (A1, A6, A9) (Supplementary Figure 3) also displaying AKR1C3 selectivity. Inhibition of intracellular AKR1C3 activity as measured using a  $11\beta$ -PGD<sub>2</sub>-ketoreductase TLC assay for representative inhibitors in each of these classes identified low nM IC<sub>50</sub> values (3–68 nM) clearly demonstrating the effective penetration of these agents into cells (Figure 6A). Despite this, these agents again did not recapitulate the combinatorial anti-leukaemic activity with BEZ displayed by the pan-AKR inhibitor MPA (Figure 6B).

At first sight these new observations appear to contradict our previous observations that overexpression of AKR1C3 demotes HL-60 differentiation in response to ATRA and that indomethacin and MPA demonstrably inhibit AKR1C3 in AML cells and exert anti-leukaemic activity (Desmond *et al*, 2003; Khanim *et al*, 2009a). However, we have reported that AML cells variably co-express AKR1-C1, -1C2 and -1C3 (Birtwistle *et al*, 2009). We have also demonstrated that both jasmonic acid and methyl jasmonate, which inhibited AKR1C2 and -1C3 predominantly but also had had some activity against AKR1C1 and -1C4, were sufficient to promote apoptosis and/or differentiation in leukaemia cell (Davies *et al*, 2009). A unifying explanation would be that the leukaemic properties of AML cells are reinforced by the combined activity of these enzymes and that pan-inhibitors are required to circumvent this. In this regard our screens of the NCI diversity set identified a compound, NCI-pan inhibitor (NCI-PI) that at 10  $\mu$ M exhibited inhibitory activities against AKR1C1 -1C2 and -1C3. When used at 25  $\mu$ M this compound faithfully recapitulated the anti-leukaemic actions of MPA against HL-60 and K562 (Figure 7A and B).

## DISCUSSION

These studies have identified 4-MDDT, a novel tetracycline breakdown product, as an excellent lead compound for the development of a specific AKR1C3 inhibitor. 4-MDDT was able to

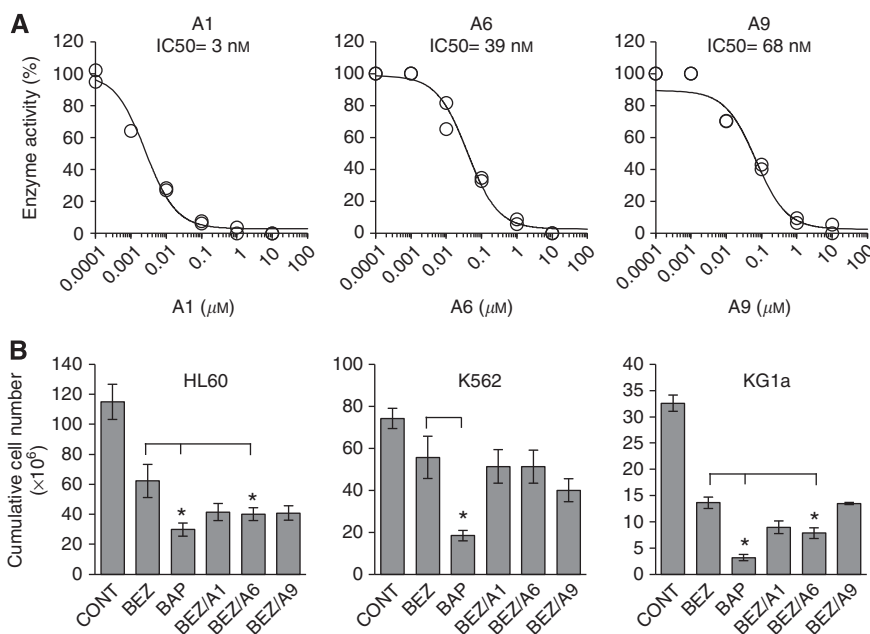


**Figure 6.** AKR1C3-selective inhibitors from CRT also do not recapitulate the cellular effects of MPA. **(A)** Dose titrations of A1, A6 or A9 were used to determine the IC<sub>50</sub> of the selected CRT compounds, for recombinant AKR1C3 protein as determined using the PQ assay (see Materials and Methods). **(B)** Cumulative cell counts for HL60, K562 and KG1a after 7 days treatment with either solvent control, 0.5 mM BEZ, BAP (0.5 mM BEZ + 5  $\mu$ M MPA), or 10  $\mu$ M A1/A6/A9 with 0.5 mM BEZ. Data shown is mean of a minimum of  $N=3$  experiments  $\pm$  s.e.m. \* $P<0.01$ .



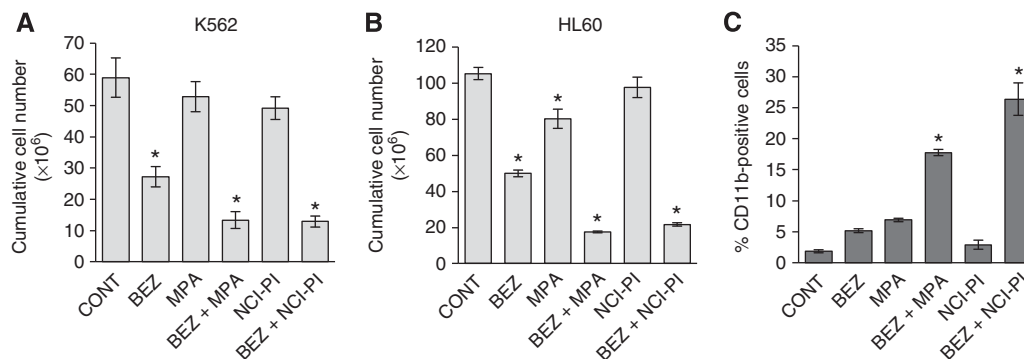


**Figure 7.** A pan-AKR1C inhibitor NCI-PI recapitulates the cellular effects of MPA. **(A and B)** Cumulative cell counts for HL60 and K562 after 7 days treatment with either solvent control, 0.5 mM BEZ, 5  $\mu$ M MPA, BaP (0.5 mM BEZ + 5  $\mu$ M MPA), 25  $\mu$ M NCI-PI alone and 25  $\mu$ M NCI-PI + 0.5 mM BEZ. **(C)** HL60 differentiation was assessed at day 7 by staining for CD11b and flow cytometry following treatments as above. Data shown is mean of a minimum of  $N=3$  experiments  $\pm$  s.e.m. \* $P<0.01$ .

inhibit AKR1C3 enzyme activity in both recombinant enzyme assays and also in intact cells (Figures 1C and 3E). The relationship to a widely used antibiotic identifies this compound as a candidate for hit-to-lead development alongside the development of indomethacin-based analogues (Byrns *et al*, 2012; Liedtke *et al*, 2013). In parallel, alternative strategies using two different assays systems and compound libraries identified a further seven AKR1C3-selective inhibitors (Figures 5A and 6) with IC<sub>50</sub> values against recombinant AKR1C3 protein ranging from 3 nM to  $\sim$ 25  $\mu$ M. The structures of the NCI and CRT compounds are highly diverse, although all of them have at least 1  $\times$  6-carbon ring (Supplementary Figures 2 and 3).

Despite these inhibitory activities against recombinant AKR1C3 protein in biochemical assays, our *in vitro* cell data indicates that, at least in AML and CLL, a selective AKR1C3 agent has no or little anti-neoplastic activity, as none of the inhibitors reduced cell proliferation, increased differentiation or induced apoptosis in our cell models. This has significant implications for the development of AKR1C3 inhibitors as anti-neoplastic agents and highlights the need to have biological assays integrated into drug development strategies.

In contrast, the pan AKR1C1, -1C2 and -1C3 inhibitor NCI-PI faithfully recapitulated the actions of MPA. Given that the chemical structure of NCI-PI is dissimilar to MPA, it appears likely that the shared anti-leukaemic actions of these compound are mediated by their shared ability to inhibit AKR1C isoforms rather than other shared 'off-target' effects. This argument is further reinforced by similar anti-leukaemic actions of other structurally diverse AKR1C inhibitors including indomethacin and jasmonates (Desmond *et al*, 2003).

Although not immediately tractable as an anti-leukaemic agent, the availability of 4-MDDT as a research tool will enable investigators interested in other disease settings to ascertain whether selective AKR1C3 inhibitors have potential utility and for studies of the biology of AKR1C3 in various cells. For example, it will be interesting to test whether 4-MDDT or any of the other identified AKR1C3-selective inhibitors can restore sensitivity to anticancer drugs, such as doxorubicin and oracin and cisplatin, where AKR1C3 has been shown to contribute to the development of drug resistance (Adegoke and Nyokong, 2012; Adegoke *et al*, 2012a, b).

In summary, we demonstrate that 4-MDDT provides an excellent lead structure with proven drug-like qualities, pharmacokinetics and toxicity profile for the development of AKR1C3 inhibitors. However, our findings suggest that, at least in AML, selective inhibition of AKR1C3 is insufficient to elicit an anticancer effect.

## ACKNOWLEDGEMENTS

We would like to thank Dr Peter Ashton (School of Chemistry, University of Birmingham) for help with mass spectrometry analysis and Laura Cronin (School of Biosciences, University of Birmingham) for help with manuscript preparation. This research was funded by grant support from Leukaemia and Lymphoma Research (LLR).

## CONFLICT OF INTEREST

The authors declare no conflict of interest.

## REFERENCES

- Adegoke O, Kulasingam S, Virnig B (2012a) Cervical cancer trends in the United States: a 35-year population-based analysis. *J Womens Health (Larchmt)* **21**(10): 1031–1037.
- Adegoke O, Nyokong T (2012) A comparative study on the sensitive detection of hydroxyl radical using thiol-capped CdTe and CdTe/ZnS quantum dots. *J Fluoresc* **22**(6): 1513–1519.
- Adegoke OA, Ghosh M, Mukherjee A (2012b) Spectrophotometric and thermodynamic studies of the interactions of 4-carboxyl-2,6-dinitrophenylazohydroxynaphthalenes with bovine serum albumin. *Spectrochim Acta A Mol Biomol Spectrosc* **96**: 1038–1046.
- Adegoke OA, Kyu JK, Mukherjee A (2012c) In vitro genotoxicity evaluation of 4-carboxyl-2,6-dinitrophenylazohydroxynaphthalenes using human lymphocytes. *Food Chem Toxicol* **50**(3–4): 936–941.
- Aderibigbe SA, Adegoke OA, Idowu OS, Olalaye SO (2012) Sensitive spectrophotometric determination of aceclofenac following azo dye formation with 4-carboxyl-2,6-dinitrobenzene diazonium ion. *Acta Pol Pharm* **69**(2): 203–211.
- Agung B, Otoi T, Abe H, Hoshi H, Murakami M, Karja NW, Murakami MK, Wongsrikeao P, Watari H, Suzuki T (2005) Relationship between oxygen consumption and sex of bovine in vitro fertilized embryos. *Reprod Domest Anim* **40**(1): 51–56.
- Bagga R, Jain V, Das CP, Gupta KR, Gopalan S, Malhotra S (2005) Choice of therapy and mode of delivery in idiopathic intracranial hypertension during pregnancy. *MedGenMed* **7**(4): 42.
- Bauman DR, Steckelbroeck S, Penning TM (2004) The roles of aldo-keto reductases in steroid hormone action. *Drug News Perspect* **17**(9): 563–578.
- Beckmann L, Husing A, Setiawan VW, Amiano P, Clavel-Chapelon F, Chanock SJ, Cox DG, Diver R, Dossus L, Feigelson HS, Haiman C, Hallmans G, Hayes RB, Henderson BE, Hoover RN, Hunter DJ, Khaw K, Kolonel LN, Kraft P, Lund E, Le Marchand L, Peeters PH, Riboli E, Stram D, Thomas G, Thun MJ, Tumino R, Trichopoulos D, Vogel U, Willett WC, Yeager M, Ziegler R, Hankinson SE, Kaaks R (2011)

- Comprehensive analysis of hormone and genetic variation in 36 genes related to steroid hormone metabolism in pre- and postmenopausal women from the breast and prostate cancer cohort consortium (BPC3). *J Clin Endocrinol Metab* **96**(2): E360–E367.
- Birtwistle J, Hayden RE, Khanim FL, Green RM, Pearce C, Davies NJ, Wake N, Schrewe H, Ride JP, Chipman JK, Bunce CM (2009) The aldo-keto reductase AKR1C3 contributes to 7,12-dimethylbenz(a)anthracene-3,4-dihydrodiol mediated oxidative DNA damage in myeloid cells: implications for leukemogenesis. *Mutat Res* **662**(1–2): 67–74.
- Bunce CM, French PJ, Durham J, Stockley RA, Michell RH, Brown G (1994) Indomethacin potentiates the induction of HL60 differentiation to neutrophils, by retinoic acid and granulocyte colony-stimulating factor, and to monocytes, by vitamin D3. *Leukemia* **8**(4): 595–604.
- Burnett AK, Russell NH, Hills RK, Kell J, Freeman S, Kjeldsen L, Hunter AE, Yin J, Craddock CF, Dufva IH, Wheatley K, Milligan D (2012) Addition of gemtuzumab ozogamicin to induction chemotherapy improves survival in older patients with acute myeloid leukemia. *J Clin Oncol* **30**(32): 3924–3931.
- Byrns MC, Mindnich R, Duan L, Penning TM (2012) Overexpression of aldo-keto reductase 1C3 (AKR1C3) in LNCaP cells diverts androgen metabolism towards testosterone resulting in resistance to the 5 $\alpha$ -reductase inhibitor finasteride. *J Steroid Biochem Mol Biol* **130**(1–2): 7–15.
- Byrns MC, Penning TM (2009) Type 5 17 $\beta$ -hydroxysteroid dehydrogenase/prostaglandin F synthase (AKR1C3): role in breast cancer and inhibition by non-steroidal anti-inflammatory drug analogs. *Chem Biol Interact* **178**(1–3): 221–227.
- Davies NJ, Hayden RE, Simpson PJ, Birtwistle J, Mayer K, Ride JP, Bunce CM (2009) AKR1C isoforms represent a novel cellular target for jasmonates alongside their mitochondrial-mediated effects. *Cancer Res* **69**(11): 4769–4775.
- Desmond JC, Mountford JC, Drayson MT, Walker EA, Hewison M, Ride JP, Luong QT, Hayden RE, Vanin EF, Bunce CM (2003) The aldo-keto reductase AKR1C3 is a novel suppressor of cell differentiation that provides a plausible target for the non-cyclooxygenase-dependent antineoplastic actions of nonsteroidal anti-inflammatory drugs. *Cancer Res* **63**(2): 505–512.
- Deyashiki Y, Ogasawara A, Nakayama T, Nakanishi M, Miyabe Y, Sato K, Hara A (1994) Molecular cloning of two human liver 3 $\alpha$ -hydroxysteroid/dihydrodiol dehydrogenase isoenzymes that are identical with chlordecone reductase and bile-acid binder. *Biochem J* **299**(Pt 2): 545–552.
- Dufort I, Soucy P, Labrie F, Luu-The V (1996) Molecular cloning of human type 3 $\alpha$  3 $\alpha$ -hydroxysteroid dehydrogenase that differs from 20 $\alpha$ -hydroxysteroid dehydrogenase by seven amino acids. *Biochem Biophys Res Commun* **228**(2): 474–479.
- Feng C, Beller EM, Bagga S, Boyce JA (2006) Human mast cells express multiple EP receptors for prostaglandin E2 that differentially modulate activation responses. *Blood* **107**(8): 3243–3250.
- Ghia P, Guida G, Gottardi D, Geuna M, Strola G, Scielzo C, Caligaris-Cappio F (2003) The pattern of CD38 expression defines a distinct subset of chronic lymphocytic leukemia (CLL) patients at risk of disease progression. *Blood* **101**(4): 1262–1269.
- Giebel S, Labopin M, Mohty M, Mufti GJ, Niederwieser D, Cornelissen JJ, Janssen JJ, Milpied N, Vindelov L, Petersen E, Arnold R, Bacigalupo A, Blaise D, Craddock C, Nagler A, Frasson F, Sadus-Wojciechowska M, Rocha V (2013) The impact of center experience on results of reduced intensity: allogeneic hematopoietic SCT for AML. An analysis from the Acute Leukemia Working Party of the EBMT. *Bone Marrow Transplant* **48**(2): 238–242.
- Gratacos-Cubarsi M, Fernandez-Garcia A, Picouet P, Valero-Pamplona A, Garcia-Regueiro JA, Castellari M (2007) Formation of tetracycline degradation products in chicken and pig meat under different thermal processing conditions. *J Agr Food Chem* **55**(11): 4610–4616.
- Guan KL, Xiong Y (2011) Regulation of intermediary metabolism by protein acetylation. *Trends Biochem Sci* **36**(2): 108–116.
- Halling-Sorensen B, Sengelov G, Tjornelund J (2002) Toxicity of tetracyclines and tetracycline degradation products to environmentally relevant bacteria, including selected tetracycline-resistant bacteria. *Arch Environ Con Tox* **42**(3): 263–271.
- Hayden RE, Pratt G, Davies NJ, Khanim FL, Birtwistle J, Delgado J, Pearce C, Sant T, Drayson MT, Bunce CM (2009) Treatment of primary CLL cells with bezafibrate and medroxyprogesterone acetate induces apoptosis and represses the pro-proliferative signal of CD40-ligand, in part through increased 15dDelta12,14,PGJ2. *Leukemia* **23**(2): 292–304.
- Hayden RE, Pratt G, Drayson MT, Bunce CM (2010) Lycorine sensitizes CD40 ligand-protected chronic lymphocytic leukemia cells to bezafibrate and medroxyprogesterone acetate-induced apoptosis but dasatinib does not overcome reported CD40-mediated drug resistance. *Haematologica* **95**(11): 1889–1896.
- Hebert AS, Dittenhafer-Reed KE, Yu W, Bailey DJ, Selen ES, Boersma MD, Carson JJ, Tonelli M, Balloon AJ, Higbee AJ, Westphall MS, Pagliarini DJ, Prolla TA, Assadi-Porter F, Roy S, Denu JM, Coon JJ (2013) Calorie restriction and SIRT3 trigger global reprogramming of the mitochondrial protein acetylome. *Mol Cell* **49**(1): 186–199.
- Hofland J, van Weerden WM, Dits NF, Steenbergen J, van Leenders GJ, Jenster G, Schroder FH, de Jong FH (2010) Evidence of limited contributions for intratumoral steroidogenesis in prostate cancer. *Cancer Res* **70**(3): 1256–1264.
- Houghton PJ, Lock R, Carol H, Morton CL, Phelps D, Gorlick R, Kolb EA, Keir ST, Reynolds CP, Kang MH, Maris JM, Wozniak AW, Gu Y, Wilson WR, Smith MA (2011) Initial testing of the hypoxia-activated prodrug PR-104 by the pediatric preclinical testing program. *Pediatr Blood Cancer* **57**(3): 443–453.
- Izumoto S, Suzuki T, Kinoshita M, Hashiba T, Kagawa N, Wada K, Fujimoto Y, Hashimoto N, Saitoh Y, Maruno M, Yoshimine T (2005) Immunohistochemical detection of female sex hormone receptors in craniopharyngiomas: correlation with clinical and histologic features. *Surg Neurol* **63**(6): 520–525.
- Jamieson SM, Brooke DG, Heinrich D, Atwell GJ, Silva S, Hamilton EJ, Turnbull AP, Rigoreau LJ, Trivier E, Soudy C, Samlal SS, Owen PJ, Schroeder E, Raynham T, Flanagan JU, Denny WA (2012) 3-(3,4-Dihydroisoquinolin-2(1H)-ylsulfonyl)benzoic Acids: highly potent and selective inhibitors of the type 5 17 $\beta$ -hydroxysteroid dehydrogenase AKR1C3. *J Med Chem* **55**(17): 7746–7758.
- Khanim FL, Hayden RE, Birtwistle J, Lodi A, Tiziani S, Davies NJ, Ride JP, Viant MR, Gunther UL, Mountford JC, Schrewe H, Green RM, Murray JA, Drayson MT, Bunce CM (2009a) Combined bezafibrate and medroxyprogesterone acetate: potential novel therapy for acute myeloid leukaemia. *PLoS One* **4**(12): e8147.
- Khanim FL, Hayden RE, Birtwistle J, Lodi A, Tiziani S, Davies NJ, Ride JP, Viant MR, Gunther UL, Mountford JC, Schrewe H, Green RM, Murray JA, Drayson MT, Bunce CM (2009b) Combined bezafibrate and medroxyprogesterone acetate: potential novel therapy for acute myeloid leukaemia. *PLoS One* **4**(12): e8147.
- Kuhne M, Korner U, Wenzel S (2001) Tetracycline residues in meat and bone meals. Part 2: The effect of heat treatments on bound tetracycline residues. *Food Addit Contam* **18**(7): 593–600.
- Li ZS, Wang W, Liao Z, Zou DW, Jin ZD, Chen J, Wu RP, Liu F, Wang LW, Shi XG, Yang Z, Wang L (2010) A long-term follow-up study on endoscopic management of children and adolescents with chronic pancreatitis. *Am J Gastroenterol* **105**(8): 1884–1892.
- Liedtke AJ, Adeniji AO, Chen M, Byrns MC, Jin Y, Christianson DW, Marnett LJ, Penning TM (2013) Development of potent and selective indomethacin analogues for the inhibition of AKR1C3 (Type 5 17 $\beta$ -hydroxysteroid dehydrogenase/prostaglandin F synthase) in castrate-resistant prostate cancer. *J Med Chem* **56**(6): 2429–2446.
- Loving AL, Ride JP, Bunce CM, Desmond JC, Cummings SM, White SA (2004) Crystal structures of prostaglandin D(2) 11-ketoreductase (AKR1C3) in complex with the nonsteroidal anti-inflammatory drugs flufenamic acid and indomethacin. *Cancer Res* **64**(5): 1802–1810.
- Matsuura K, Shiraishi H, Hara A, Sato K, Deyashiki Y, Ninomiya M, Sakai S (1998) Identification of a principal mRNA species for human 3 $\alpha$ -hydroxysteroid dehydrogenase isoform (AKR1C3) that exhibits high prostaglandin D2 11-ketoreductase activity. *J Biochem (Tokyo)* **124**(5): 940–946.
- Mitsiades N, Sung CC, Schultz N, Danila DC, He B, Eedunuri VK, Fleisher M, Sander C, Sawyers CL, Scher HI (2012) Distinct patterns of dysregulated expression of enzymes involved in androgen synthesis and metabolism in metastatic prostate cancer tumors. *Cancer Res* **72**(23): 6142–6152.
- Morakinyo AO, Iranloye BO, Daramola AO, Adegoke OA (2011) Antifertility effect of calcium channel blockers on male rats: association with oxidative stress. *Adv Med Sci* **56**(1): 95–105.
- Murray JA, Khanim FL, Hayden RE, Craddock CF, Holyoake TL, Jackson N, Lumley M, Bunce CM, Drayson MT (2010) Combined bezafibrate and medroxyprogesterone acetate have efficacy without haematological

- toxicity in elderly and relapsed acute myeloid leukaemia (AML). *Br J Haematol* **149**(1): 65–69.
- Patriciu A, Mazilu D, Petrisor D, Bagga H, Kavoussi L, Stoianovici D (2005) A computer assisted method for guide-wire and catheter evaluation. *Conf Proc IEEE Eng Med Biol Soc I*: 436–439.
- Qiu W, Zhou M, Mazumdar M, Azzi A, Ghanmi D, Luu-The V, Labrie F, Lin SX (2007) Structure-based inhibitor design for an enzyme that binds different steroids: a potent inhibitor for human type 5 17 $\beta$ -hydroxysteroid dehydrogenase. *J Biol Chem* **282**(11): 8368–8379.
- Richards SM, Jensen RV, Liu M, Sullivan BD, Lombardi MJ, Rowley P, Schirra F, Treister NS, Suzuki T, Steagall RJ, Yamagami H, Sullivan DA (2006) Influence of sex on gene expression in the mouse lacrimal gland. *Exp Eye Res* **82**(1): 13–23.
- Rizner TL, Penning TM (2013) Role of aldo-keto reductase family 1 (AKR1) enzymes in human steroid metabolism. *Steroids* **79C**: 49–63.
- Suzuki T, Miki Y, Nakamura Y, Moriya T, Ito K, Ohuchi N, Sasano H (2005) Sex steroid-producing enzymes in human breast cancer. *Endocr Relat Cancer* **12**(4): 701–720.
- Velica P, Davies NJ, Rocha PP, Schrewe H, Ride JP, Bunce CM (2009) Lack of functional and expression homology between human and mouse aldo-keto reductase 1C enzymes: implications for modelling human cancers. *Mol Cancer* **8**: 121.
- Wang Q, Zhang Y, Yang C, Xiong H, Lin Y, Yao J, Li H, Xie L, Zhao W, Yao Y, Ning ZB, Zeng R, Xiong Y, Guan KL, Zhao S, Zhao GP (2010) Acetylation of metabolic enzymes coordinates carbon source utilization and metabolic flux. *Science* **327**(5968): 1004–1007.
- Wasylishen AR, Kalkat M, Kim SS, Pandya A, Chan PK, Oliveri S, Sedivy E, Konforte D, Bros C, Raught B, Penn LZ (2013) MYC activity is negatively regulated by a C-terminal lysine cluster. *Oncogene* **33**: 1066–1072.
- Wu RP, Hayashi T, Cottam HB, Jin G, Yao S, Wu CC, Rosenbach MD, Corr M, Schwab RB, Carson DA (2010) Nrf2 responses and the therapeutic selectivity of electrophilic compounds in chronic lymphocytic leukemia. *Proc Natl Acad Sci USA* **107**(16): 7479–7484.
- Zargar S, Moreira TS, Samimi-Seisan H, Jeganathan S, Kakade D, Islam N, Campbell J, Adegoke OA (2011) Skeletal muscle protein synthesis and the abundance of the mRNA translation initiation repressor PDCD4 are inversely regulated by fasting and refeeding in rats. *Am J Physiol Endocrinol Metab* **300**(6): E986–E992.

This work is published under the standard license to publish agreement. After 12 months the work will become freely available and the license terms will switch to a Creative Commons Attribution-NonCommercial-Share Alike 3.0 Unported License.

Supplementary Information accompanies this paper on British Journal of Cancer website (<http://www.nature.com/bjc>)